Thermochimica Acta 321 (1998) 89–98

thermochimica
acta

Poly(3-D(-)hydroxybutyrate)/atactic poly(methylmethacrylate) blends: Morphology, miscibility and crystallization relationships

S. Cimmino, P. Iodice, E. Martuscelli, C. Silvestre*

Istituto di Ricerca e Tecnologia delle Materie Plastiche, CNR, Via Toiano, 6, Arco Felice, 80072 Naples, Italy

Received 8 April 1997; accepted 1 December 1997

Abstract

The morphology, the phase structure and the crystallization processes of poly(3-D(-)hydroxybutyrate)/atactic poly(methylmethacrylate) blends, (PHB/aPMMA), have been investigated as a function of blend composition and thermal treatments. The two-phase separation processes (liquid/liquid demixing and liquid/solid separation) are in competition between each other.

In the melt at $T \geq 185°C$, the system was homogeneous. During crystallization from the melt, liquid/liquid phase separation occurred before crystallization. After crystallization, three phases were present: a crystalline PHB phase; and two amorphous phases, one formed by amorphous PHB and the other by aPMMA. From the homogeneous glass state, however, crystallization preserved the homogeneity. The system, after cold crystallization, was composed of two phases: a crystalline; and an amorphous homogeneous phase. The addition of aPMMA always caused a decrease of the spherulite radial growth and overall crystallization rates. These results are attributed to the increase of energy related to the transport of the macromolecules in the melt, and in the case of cold crystallized samples, also to the diluent effect of aPMMA on the growth of PHB crystals. © 1998 Elsevier Science B.V.

Keywords: Atactic poly(methylmethacrylate) blends; Crystallization; Morphology; Phase structure; Poly(3-D(-)hydroxybutyrate); Thermal behavior

1. Introduction

Recently, the poly(3-D(-)hydroxybutyrate)/atactic poly(methylmethacrylate) (PHB/aPMMA) system was investigated by Cimmino et al. [1]. They found that the PHB/aPMMA blends present an upper critical solution temperature (UCST) behaviour. For the 90/10 to 30/70 PHB/aPMMA blends, the UCST ranges between 170° and 185°C, whereas for the 20/80 and 10/90 blends the UCST is between 155 and 170°C. At T>UCST, the PHB and the aPMMA are completely miscible for any blend composition; conversely, at lower temperatures the melt phase separates into the two practically pure components. Moreover, it was found that the phase structure is dependent on cooling rate and composition. In fact, using a quasi-instantaneous quenching from the one phase region to a temperature lower than T_g, an amorphous homogeneous glassy material resulted, whereas with a lower cooling rate a material presenting two amorphous phases was obtained.

The discussion on phase structure [1] was limited to the amorphous phase. As the PHB is a semicrystalline

---

*Corresponding author. Tel.: +39 81 8534174; fax: +39 81 8663378; e-mail: silv@mail.irtemp.na.cnr.it

PII: S0040-6031(98)00444-4

polymer, during cooling, besides the liquid/liquid demixing a liquid/solid separation can occur because of the crystallization of PHB.

The present work aims at completing the study on PHB/aPMMA blends. It analyzes the possible competition between the two demixing processes, the melting behavior, crystallization kinetics, and the phase structure and morphology developments of the PHB/aPMMA blends as a function of T_c. The study uses thermal analysis and microscopic observation.

2. Experimental

2.1. Materials

The polymers used were poly(3-D(-)hydroxybutyrate), PHB, (ICI) with $M_w=1.59\times10^5$ and $M_w/M_n=3.2$ and atactic poly(methylmethacrylate), aPMMA, (BDH) with $M_v=1.16\times10^5$ and $M_w/M_n=3$.

2.2. Preparation of blends

The PHB/aPMMA blends of weight ratios 100/0, 90/10, 80/20 and 60/40 were prepared by solution casting from chloroform. After the precipitation, the blends were kept in a vacuum oven at 70°C for 8 h.

2.3. Calorimetric measurements

A differential scanning calorimeter (Mettler DSC 30) was used to determine the thermal properties and the crystallization kinetics of the blends. *Crystallization from the melt* was studied by using the following procedure: the sample was heated from 30° to 200°C at 10°C/min and held for 1 min at 200°C, then it was quenched to T_c and held at this temperature for a time sufficient to allow crystallization. *Crystallization from the cold* was studied by using the following procedure: the sample was heated from 30° to 200°C at 10°C/min and held for 1 min at 200°C, thereafter quenched at 100°C/min to −50°C, then it was heated at 10°C/min to T_c where it was allowed to isothermally crystallize.

The heat evolved during the crystallization was recorded as a function of time. The weight fraction X_t of the material crystallized at time t was calculated from the ratio of the heat generated at time t and the total heat corresponding to the completion of crystallization. Plotting X_t against time, the half-time of crystallization, $\tau_{1/2}$, defined as the time taken for half of the crystallinity to develop, was obtained.

After crystallization, all the samples were melted at 200°C with a heating rate of 10°C/min.

The times and temperatures were chosen in order to limit the thermal degradation of PHB [2].

2.4. Optical and electron microscopy

The morphology of the blends and the growth rate of PHB spherulites in the blends as a function of crystallization temperature, composition and blend preparation were analyzed by optical and electron microscopy, using a Zeiss polarizing microscope equipped with a hot-stage and a SEM 501 Philips microscope on cryogenically fractured surfaces of samples of PHB/aPMMA blends. Before the electron microscopy observation, the surfaces were coated with Au–Pd alloy with an SEM coating device (SEM Coating Unit E5150 – Polaron).

The radial growth rate, $G=dR/dt$ (where R is the radius of spherulites and t the time), was calculated by measuring the size of PHB spherulites during the isothermal crystallization process. The standard procedure was the following: the sample was sandwiched between two microscope slides, heated at 200°C for 1 min. The temperature was then rapidly lowered to T_c and the sample allowed to crystallize. The radial growth rate of a spherulite focused upon was finally monitored during crystallization by taking photomicrographs at appropriate intervals of time: G was calculated as the slope of the straight lines resulting from plots of R against time.

3. Results and discussion

3.1. Morphology and phase structure

Optical and electron microscopy highlighted that the overall morphology and the phase structure depend on temperature, crystallization conditions and composition.

In the melt, at 200°C, for all the blends there was no evidence of aPMMA domains segregated in a PHB matrix, indicating that the two polymers are miscible

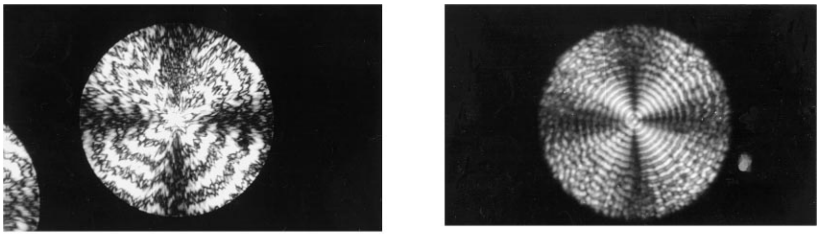

a) PHB **b) PHB/aPMMA 90/10**

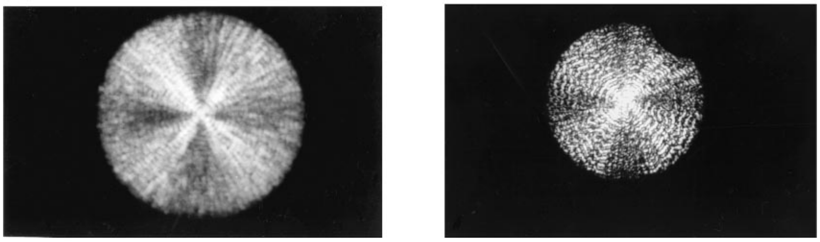

c) PHB/aPMMA 80/20 **d) PHB/PMMA 60/40**

Fig. 1. Optical micrograph of PHB/aPMMA blends isothermally crystallized at T_c=120°C: (a) 100/0; (b) 90/10; (c) 80/20; and (d) 60/40.

at this temperature. This is in agreement with the phase diagram [1].

The overall morphology of the melt changes when the temperature drops below 170°C. Before the crystallization of PHB, it was possible to see small spherical domains homogeneously distributed in all samples. Previously [1], it was reported that the samples annealed at 170° and 140°C presented two distinct glass-transition temperatures, whose values were constant with composition and similar to those of the pure components. This result, together with the morphological evidences reported above, probably indicates that during the cooling the system practically separates in the two pure components and that the phase separation process precedes the crystallization phenomenon. Therefore, in blends, the PHB crystallized in equilibrium with a non-homogeneous melt. During the crystallization, the aPMMA domains were occluded in the growing spherulites. At the end of the crystallization process, the system was constituted of three phases: one crystalline PHB phase, one amorphous PHB phase, probably located among the lamellae of the PHB crystals, and a phase constituted of aPMMA mainly present in the intraspherulitic regions of PHB crystals.

The PHB always crystallized from the melt in a spherulitic morphology, characterized by the presence of concentric rings (Figs. 1 and 2). From electron micrographs it seems, moreover, that the PHB spherulites have a hedritic character. In fact, terraces, which according to Mandelkern et al. [3] are characteristic of a hedritic morphology, are always present, as can be seen, for example, in Fig. 3.

The shape and the dimensions of spherulites, the regularity and periodicity of the rings depend on crystallization temperature and composition.

For all samples, the number of spherulites per unit of area decreased with an increase of temperature, according to the kinetic theory of polymer crystallization [4,5], which predicts a decrease of nucleation rate with crystallization temperature. The number of nuclei per unit area (nucleation density), for a given temperature, is dependent on composition, as can be seen from the optical micrographs, (Figs. 1 and 2). At a higher crystallization temperature, (T_c=120°C), the nucleation density is almost independent of composition (Fig. 1). At lower crystallization temperatures (T_c=70°C) instead, it was observed that the nucleation density increased with increase of aPMMA content, suggesting that aPMMA at this temperature behaves as a nucleating agent for PHB (Fig. 2). The different influences of aPMMA on PHB nucleation, with crystallization temperature, are probably connected with the different physical states of the amorphous

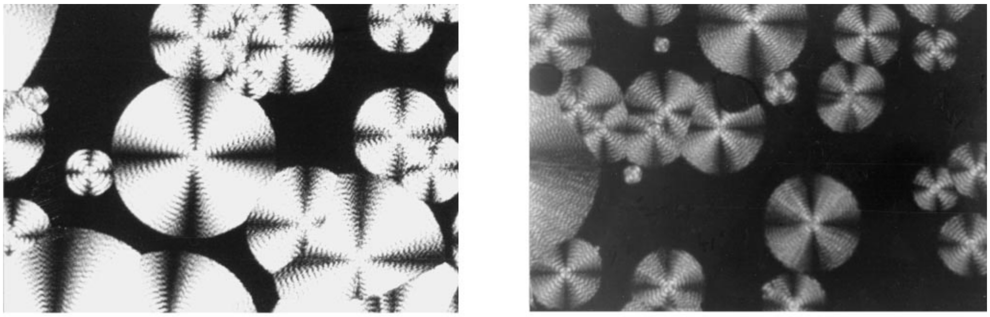

a) PHB

b) PHB/aPMMA 90/10

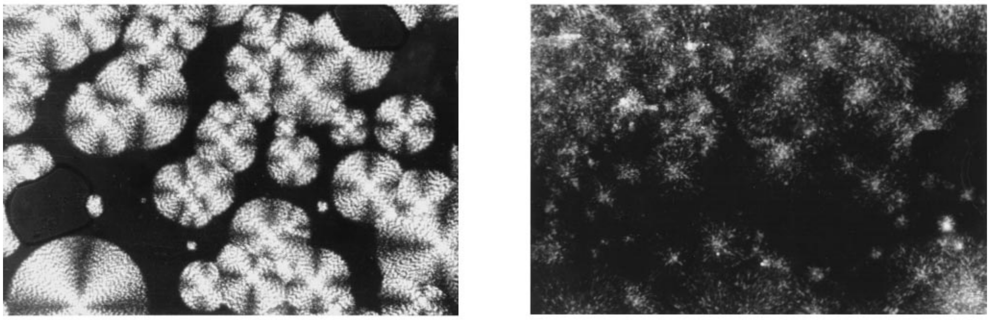

c) PHB/aPMMA 80/20

d) PHB/PMMA 60/40

Fig. 2. Optical micrograph of PHB/aPMMA blends isothermally crystallized at T_c=70°C: (a) 100/0; (b) 90/10; (c) 80/20; and (d) 60/40.

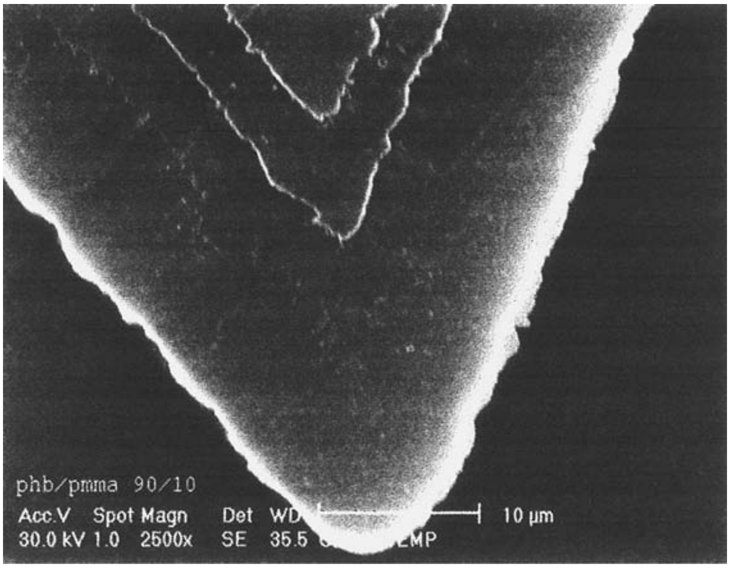

Fig. 3. Electron micrograph of PHB/aPMMA 90/10 isothermally crystallized at T_c=110°C from the melt state.

polymer. In fact, at 70°C the aPMMA phase is in the glassy state, whereas at 120°C it is in the rubbery state. At 70°C, the glassy aPMMA domains present sharper contact surfaces that seem to promote the nucleation of PHB, [6,7]. Moreover, this probably can act as an epitaxial register favouring a better matching with the polymer chains [8].

The banded interference figures are influenced by composition and temperature. For PHB, numerous concentric rings appear at low T_c with a low periodicity, whereas at higher T_c the rings span out and the periodicity increases (Fig. 1(a) and Fig. 2(a)). For the blends, the situation is more complex. In fact, the periodicity of the concentric rings and their presence depend on temperature as well as on composition.

The 90/10 PHB/aPMMA blend presents concentric rings with spacing independent of crystallization temperature (Fig. 1(b) and Fig. 2(b)). The 80/20 PHB/aPMMA blend, instead, presents concentric rings clearly distinguishable at high Tc (Fig. 1(c)), whereas, at low T_c the rings are not very evident (Fig. 2(c)). Finally, the 60/40 blend at high T_c shows (Fig. 1d) neat concentric rings that are not present at low T_c (Fig. 2(d)).

The interference figure with concentric rings, according to Basset [9], is achieved by interleaving sequences of curved lamellar units, when the spherulitic growth is sufficiently quick compared with the molecular transport. For pure polymer, this condition occurs mainly at low crystallization temperatures. For the PHB/aPMMA blends, it is difficult to explain the results, as the presence of aPMMA negatively influences both the spherulitic radial growth rate and the molecular transport (see Section 3.2). Probably, the spherulitic radial growth rate and the molecular mobility do not vary in the same way with composition and temperature.

The samples quenched to −50°C from the melt are completely transparent. There is not evidence of domains of a dispersed phase or PHB crystals, suggesting that the fast cooling process preserves the homogeneity that the two polymers have in the melt and prevents the crystallization of PHB.

The PHB crystallizes on increasing the temperature. During the crystallization from the glassy state, small crystals form, whereas the uncrystallized parts of sample remain unchanged and no phase separation is observed. This hypothesis is confirmed by the absence of a glass transition relative to aPMMA phase in DSC scan.

Thus, the PHB in the blends crystallizes from the glassy state in presence of a homogeneous system. At the end of the crystallization, the blend was constituted of two phases, a PHB crystalline phase and an amorphous homogeneous phase of PHB and aPMMA. The amorphous homogeneous phase remains unchanged on annealing the sample at temperatures, where the phase diagram predicts a phase separation. This result suggests that the PHB crystallization inhibits the liquid–liquid demixing.

3.2. Crystallization kinetics

The spherulite growth rate, G, for the melt crystallized samples as a function of temperature for different blend compositions is reported in Fig. 4. A maximum in the G values was observed at ca. 90°C for the pure PHB and all blends.

For a given T_c, the addition of aPMMA to a PHB matrix caused a depression of G that is a function of composition. At the T_c investigated, the morphologic and calorimetric results showed that the blends were phase separated, so the crystallization of PHB starts from a separated melt. As already reported [10–22], the presence of a non-crystallizable material mainly influences the energy related to the transport of the macromolecules in the melt at T_c. In fact, during crystallization, the domains of the non crystallizable material may be rejected by the crystallizing front at the boundaries of the spherulites and/or they may be occluded and deformed. The presence of these domains on the path of crystallizing front can markedly disturb the crystallization. Energy must be dissipated to perform the occlusion, the deformation and the rejection. Such energies constitute a new energy barrier, that controls the growth of the spherulites. Consequently, the decrease of the radial growth rate observed for the PHB/aPMMA systems must be due, principally, to the effect of the microscopic aPMMA domains, that are included in the PHB spherulites during the crystallization, producing an increase of energy relative to the motion of the macromolecules in the melt at T_c.

The half-time of crystallization, $\tau_{1/2}$, as a function of crystallization and temperature for different blend

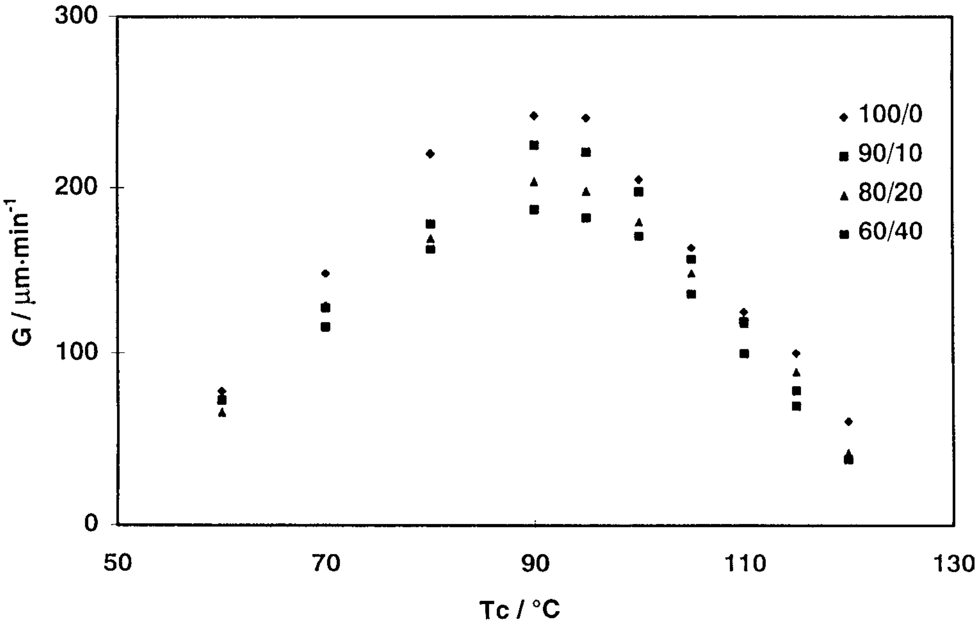

Fig. 4. Spherulitic radial growth rate as a function of T_c for PHB and PHB/aPMMA blends.

compositions is reported in Fig. 5(a–b) for melt and cold crystallization respectively.

The addition of aPMMA to PHB, for a given T_c, always causes a decrease in the overall crystallization rate. The entity of this depression is a function of T_c and crystallization conditions: for melt crystallized samples a marked increase of $\tau_{1/2}$ with composition is observed at higher T_cs, whereas, at lower temperature (80–90°C) $\tau_{1/2}$ is almost constant with composition (see Fig. 5(a)); for the cold crystallized samples, an opposite trend is shown (see Fig. 5(b)). In fact, the increase of the half-time of crystallization with composition observed at low T_cs becomes less pronounced at increasing T_c values (Fig. 5(b)). These results can be explained by taking into account the fact that the overall crystallization rate depends on the nucleation rate and on the radial growth rate of the spherulites. For the melt crystallized samples, the spherulitic growth rate, for all T_c, decreases with increase of aPMMA percentage in the blends. Therefore, by itself this effect should cause a decrease in the overall crystallization rate. The contribution due to nucleation, instead, is more complex and depends on composition and temperature. As reported in Section 3.1, the aPMMA at T_c below 100°C seems to act as a nucleating agent for the PHB, whereas at higher temperatures this effect disappears. On the basis of the morphological results, it is possible to conclude that, at high temperatures, the nucleation being independent of aPMMA percentage, the decrease of the overall crystallization rate with the composition must be due principally to the presence of aPMMA that disturbs the motion of the macromolecules in the melt. At low temperatures, the nucleating effect counterbalances the effect due to the transport and the final result is a crystallization rate, apparently, slightly dependent on composition (Fig. 5).

For the cold crystallization samples, it must be considered that the PHB crystallizes in equilibrium with a homogeneous system and, therefore, the decrease of overall crystallization rate is probably also due to the aPMMA diluent effect, according to the crystallization theory of miscible polymer blends [13,23].

The experimental data are analyzed using the Avrami phase transition theory [24] whose equation is written as:

$$\lg[-\ln(1-X_t)] = -\lg K + n\lg t \tag{1}$$

where X_t is the crystalline ratio at the time t, K the

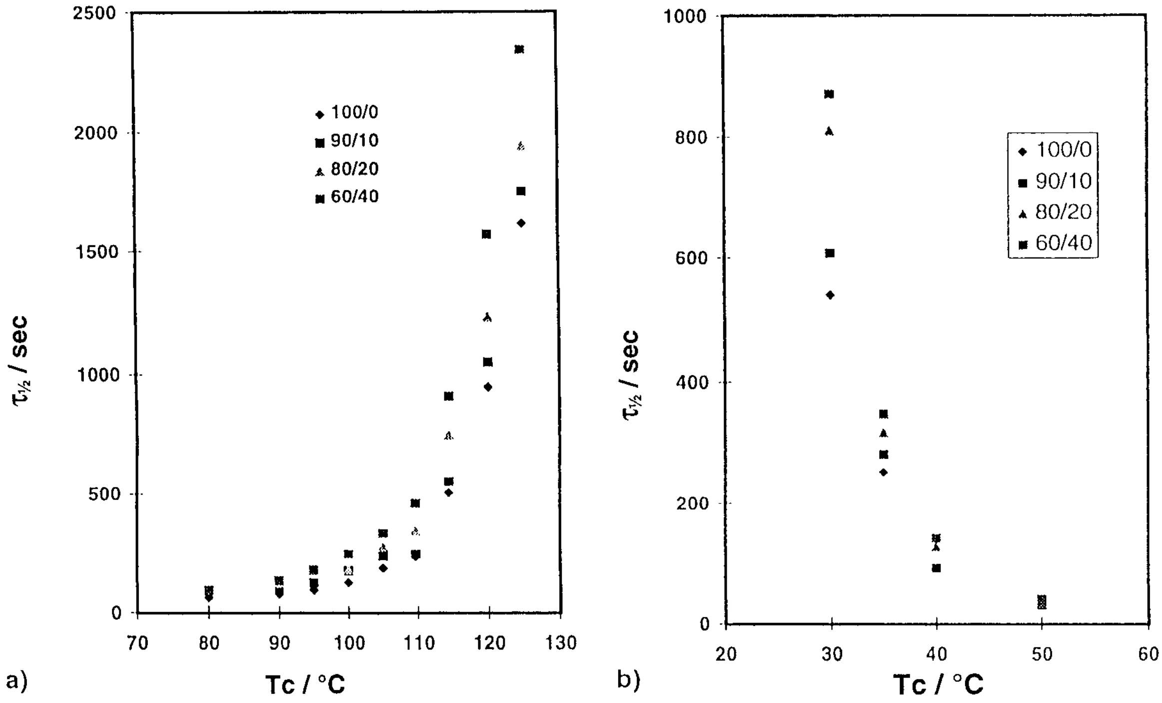

Fig. 5. Half-life of crystallization, $\tau_{1/2}$, as a function of T_c for PHB and PHB/aPMMA blends; (a) melt crystallization; and (b) cold crystallization.

overall rate constant and n the Avrami index. This equation fits well the experimental data. In fact, plotting the first term of Eq. (1) as a function of lg t, straight lines were obtained. From the slope of such straight lines, it is possible to derive a value for n. For all the samples, independent of composition and T_c, n assumes a value close to 2. Assuming a heterogeneous nucleation, both for the pure PHB and the blends, according to Avrami theory, a value of n=2 indicates a bi-dimensional growth of the crystals. On the basis of this result, it is possible to suppose, therefore, that the PHB crystal growth is predominantly bi-dimensional. This conclusion is confirmed by the morphology. The presence of terraces observable in the electron micrographs, in fact, clearly indicates a bi-dimensional growth of the crystals (Fig. 3).

3.3. Thermal behaviour

The thermal behaviour of the PHB and the PHB/aPMMA blends is dependent on the crystallization condition, composition and crystallization temperatures. For the cold crystallized samples, a single melting peak, centred at a temperature of 172°C independently of T_c and composition, is always present.

The situation is more complex for the melt crystallized samples. For the PHB and PHB/aPMMA blends, crystallized at T_c below 120°C, it is possible to observe two melting peaks. At $T_c \geq 120$°C, a single melting peak is observed (Fig. 6). The lower temperature melting peak, T_m(I), shifts to higher temperatures for samples crystallized at higher T_c, whereas T_m(II) is always centred around a value of 172°C. The trend of T_m(I) and T_m(II), with T_c, shows that the lower temperature peak is relative to the melting of crystals formed isothermally at T_c, whereas the higher temperature peak is due to the melting of crystals that undergo an annealing process during scanning.

For the samples crystallized at low temperatures (80–90°C), the scanning time from T_c to T_m is long and the annealing process can more easily happen. This process is favoured by the small dimensions of the crystalline lamellae formed at low T_c. This hypothesis is confirmed by the presence of a single melting peak in the scan of cold crystallization samples, centred at

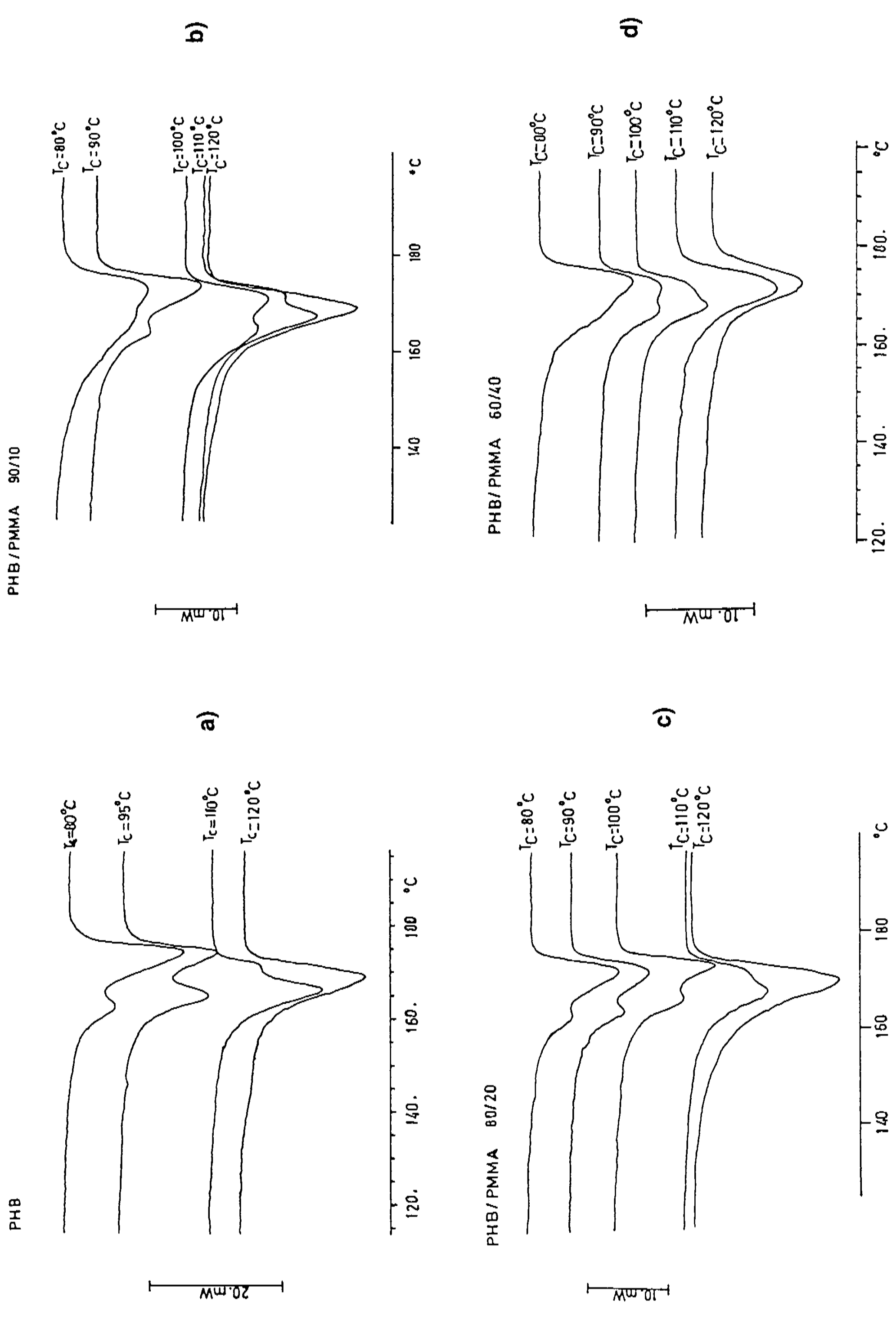

Fig. 6. DSC scans of PHB and PHB/aPMMA blends isothermally crystallized from the melt: (a) 100/0; (b) 90/10; (c) 80/20; and (d) 60/40.

172°C, that corresponds to T_m(II) of the melt crystallized samples.

The samples crystallized at high temperatures, instead, do not present double melting peaks, so the time necessary for the scanning is reduced and, at the same time, the lamellae formed at T_c are thicker and, hence, less easily suffer annealing.

To obtain the equilibrium melting temperature, T_m^0, the Hoffman and Weeks equation is generally used [25]:

$$T_m = T_m^0\left(\frac{\gamma - 1}{\gamma}\right) + \frac{T_c}{\gamma} \tag{2}$$

In Eq. (2), T_m is the observed melting point, γ is a morphologic factor, given by the ratio between the final lamella thickness and the critical one and T_m^0 the equilibrium melting temperature. According to Eq. (2), a straight line should be obtained by plotting T_m, as a function of T_c. From the intersection point of this line with the straight line $T_m = T_c$, T_m^0 could be determined.

T_m increased linearly with T_c, for both the PHB and the blends. This indicates a good fitting of experimental data with Eq. (2). The equilibrium melting points for the pure PHB and the blends are reported in Table 1.

From the table, a decrease of the equilibrium melting temperatures with composition can be observed. A decrease in T_m^0 for a blend, from a thermodynamic point of view, should indicate miscibility at the molecular level between the components in the melt at T_m^0 [26]. On the other hand, the phase structure analysis has shown that the system is immiscible in the melt at T_c; therefore, it must be concluded that the Hoffman equation cannot be used to obtain the T_m^0 value, for the PHB/aPMMA system. Probably, an annealing process, that depends on composition and scanning time, limits the use of such an equation, as already reported [27,28].

Table 1
Equilibrium melting temperatures of pure PHB and PHB/aPMMA blends obtained by using Eq. (2)

	PHB	PHB/aPMMA		
		90/10	80/20	60/40
$T_m{}^0$/°C	180	179	178	177

4. Conclusions

The results have shown that the phase structure, the morphology and the crystallization processes of PHB/aPMMA blends depend on composition, temperature, and preparation conditions. In particular, the following conclusions can be drawn:

– For all samples, in the melt at 200°C, the system is homogeneous and this situation persists if the samples are fast quenched down to −50°C. Cooling the melt at $T<170$°C, before the crystallization, the systems separate in two phases, mainly constituted by the two pure components. After the crystallization, three phases are present: one crystalline PHB and two amorphous phases.

– The crystallization and separation processes are in competition with each other. Starting from the melt, the liquid/liquid phase separation occurs before the crystallization. From the glassy state, instead, the crystallization preserves the homogeneity between the amorphous phases.

– The PHB crystallizes according to a spherulite morphology characterized by the presence of concentric rings. The spherulite shapes and dimensions depend on temperature and composition as well as on the physical state of aPMMA domains. In fact, the aPMMA, in the glassy state, behaves as a nucleating agent, whereas in the rubbery state this does not influence the nucleation process.

– The aPMMA always causes, at a given T_c, a decrease of the spherulitic radial growth rate and of the overall crystallization rate of PHB. This decrease is mainly due to the increase of energy relative to the motion of the macromolecules in the melt, caused by the presence of aPMMA domains. In the case of cold crystallization, the two components being miscible, diluent effects are also responsible for the decrease of the overall crystallization rate.

References

[1] A. Siciliano, A. Seves, T. De Marco, S. Cimmino, E. Martuscelli, C. Silvestre, Macromolecules 28 (1995) 8065.

[2] N. Grassie, E.J. Murray, P.A. Holmes, Polym. Degrad. Stab. 6 (1984) 95.

[3] R.C. Allen, L. Mandelkern, J. Polym. Sci. Polym. Phys., Ed. 20 (1982) 1465.
[4] J.D. Hoffman, G.T. Davis, J. Lauritzen, in: N.B. Hanay (Ed.), Treatise on Solid State Chemistry, Vol. 3, Chap. VI, Plenum, New York, 1976.
[5] L. Mandelkern, Crystallization of Polymers, McGraw-Hill, NY, 1964.
[6] A. Galeski, Z. Bartczak, N.P. Krasnikova, Polymer 25 (1984) 1323.
[7] A. Galeski, Z. Bartczak, E. Martuscelli, Nucleation process in toughened plastics, in: E. Martuscelli, P. Musto, G. Ragosta (Eds.), Advanced Routes for Polymer Toughening, Chap. 4, Elsevier Amsterdam, 1996, pp. 157–241.
[8] J.C. Wittmann, B. Lotz, Polymer 30 (1989) 27.
[9] C.D. Bassett, A.M. Hodge, Polymer 19 (1978) 469.
[10] E. Martuscelli, Polym. Eng. Sci. 24 (1984) 563.
[11] V.M. Nadkarni, J.P. Jog, Crystallization behaviour in polymer blends in two phase polymer systems,in: L.A. Utracki (Ed.), Progress in Polymer Science, Hanser Pub., Munich, Vienna, 1991, pp. 213–239.
[12] A. Galeski, M. Pracella, E. Martuscelli, J. Polym. Sci., Polym. Phys. 22 (1984) 739.
[13] C. Silvestre, S. Cimmino, E. Di Pace, in: J.C. Salamone (Ed.), Polymer Materials Encyclopedia, Vol. II, CRC Press, 1996, pp. 689.
[14] P. Greco, E. Martuscelli, Polymer 30 (1989) 1475.
[15] Z. Barctzak, A. Galeski, E. Martuscelli, Polym. Eng. Sci. 24 (1984) 1155.
[16] E. Martuscelli, in: S.K. De, A.K. Bhowmick (Eds.), Thermoplastic Elastomers from Rubber-Plastic Blends, Chap. II, Ellis Horwood Limited, 1990.
[17] S.N. Omenyi, A.W. Newmann, C.J. van Oss, J. App. Phys. 44 (1973) 4340.
[18] E. Martuscelli, C. Silvestre, G. Abate, Polymer 23 (1982) 229.
[19] E. Martuscelli, C. Silvestre, L. Bianchi, Polymer 24 (1983) 1458.
[20] L. Bianchi, S. Cimmino, A. Forte, R. Greco, E. Martuscelli, F. Riva, C. Silvestre, J. Mat. Sci. 20 (1985) 895.
[21] S. Cimmino, E. Di Pace, E. Martuscelli, C. Silvestre, A. Buzarovska, K. Slobodanka, Polymer Networks Blends 5(2) (1995) 63.
[22] C. Silvestre, S. Cimmino, E. Di Pace, E. Martuscelli, M. Monaco, A. Buzarovska, S. Koseva, Polymer Networks Blends 6(2) (1996) 73.
[23] J. Boon, J.M. Azcue, J. Polym. Sci., Part. A-2 6 (1968) 885.
[24] M. Avrami, J. Chem. Phys. 7 (1939) 1103.
[25] J.D. Hoffman, J.J. Weeks, J. Chem. Phys. 37 (1962) 1723.
[26] T. Nishi, T.T. Wang, Macromolecules 8 (1975) 909.
[27] G.C. Alfonso, T.P. Russell, Macromolecules 19 (1986) 1143.
[28] S. Cimmino, E. Di Pace, E. Martuscelli, C. Silvestre, Makromol. Chem. 191 (1990) 2447.